# Efficient field emission from $\alpha$-$Fe_2O_3$ nanoflakes on an atomic force microscope tip

Y. W. Zhu,[a] T. Yu, C. H. Sow,[a),b)] Y. J. Liu, and A. T. S. Wee[a)]
*Department of Physics, National University of Singapore, 2 Science Drive 3, 117542, Singapore*

X. J. Xu[c)] and C. T. Lim[c)]
*Department of Mechanical Engineering, National University of Singapore, 9 Engineering Drive 1, 117576, Singapore*

J. T. L. Thong[c)]
*Department of Electrical and Computer Engineering, National University of Singapore, 4 Engineering Drive 3, 117576, Singapore*

(Received 17 March 2005; accepted 9 June 2005; published online 7 July 2005)

Aligned arrays of flake-shaped hematite ($\alpha$-$Fe_2O_3$) nanostructure have been fabricated on an atomic force microscope (AFM) tip. They are created by simply heating an iron-coated AFM tip in ambience on a hot plate. These nanoflakes are characterized as $\alpha$-$Fe_2O_3$ single crystalline structures with tip radii as small as several nanometers and are highly effective as electron field emitters. With a vacuum gap of about 150 $\mu$m, field emission measurements of $\alpha$-$Fe_2O_3$ nanoflakes on AFM tips show a low turn-on voltage of about 400–600 V and a high current density of 1.6 A $cm^{-2}$ under 900 V. Such high emission current density is attributed to the nanoscale sharp tips of the as-grown nanoflakes. Based on the Fowler–Nordheim theory, it is demonstrated the enhancement factor of $\alpha$-$Fe_2O_3$ nanoflakes on AFM tips is comparable to that of carbon nanotubes. Our findings suggest that $\alpha$-$Fe_2O_3$ nanoflakes are potentially useful as candidates for future electron field emission devices. © *2005 American Institute of Physics*. [DOI: 10.1063/1.1991978]

One-dimensional (1D) nanostructure field emitters have stimulated much attention because of their ability to concentrate the electric field. As a typical 1D nanomaterial, carbon nanotubes (CNTs) have been investigated for field emission (FE) for many years, and a large number of laboratory works[1] and prototype devices[2] have been reported. However, besides low operation voltage and high emission current, which have been achieved in CNT field emitters, thermal stability, and environmental insensitivity are equally important in the operation of field emitters. Thus, a wide variety of other 1D nanostructures have been investigated to expand the pool of candidates for field emitters and excellent FE results have been obtained.[3] At the same time, developing a more cost-effective fabrication method is still necessary for future industrial applications. Individual CNTs have also been mounted on W tips[4] or atomic force microscope (AFM) tips[5] to fabricate point emitter or AFM probes. As the most stable iron oxide, hematite ($\alpha$-$Fe_2O_3$) is of significant scientific and technological importance due to its usage in photocatalyst,[6] gas sensor,[7] and as an unusual magnetic material.[8] Recently, $\alpha$-$Fe_2O_3$ nanowires have been fabricated by various research groups.[9] However, there has been no report on the FE properties of such an important ferrite material, possibly due to the large tip dimension of the fabricated nanowires.[9] In this letter, we report a simple method to fabricate sharp $\alpha$-$Fe_2O_3$ nanoflakes locally aligned on an AFM tip and the investigation of their FE properties.

To synthesize aligned $\alpha$-$Fe_2O_3$ nanoflakes on a substrate, a Fe film was sputtered on the substrate. In this work, silicon-based tapping mode AFM tips were placed into a radio-frequency plasma-assisted sputtering machine and the chamber was evacuated to a base pressure of $10^{-6}$ Torr. After that, Ar plasma with a power of about 100 W was induced to bombard a pure Fe (99.9%) target. The deposition lasted for 2 h under room temperature (20 °C). After sputtering, the whole AFM tip was covered with a Fe film with thickness of about 1 $\mu$m on the supporting silicon base and about 500 nm at the tip part. Subsequently, as-sputtered samples were placed onto a hotplate and heated to 300 °C in ambient conditions for 45 min. After cooling, the as-grown products were characterized using scanning electron microscopy [(SEM), JEOL JSM-6400F], transmission electron microscopy [(TEM), JEOL JEM-2010F, 200 kV] and X-ray photoelectron spectroscopy [(XPS), ESCA MK II; Mg source].

A typical SEM image of an as-grown sample is shown in Fig. 1(a), from which we can see the whole surface of the AFM tip uniformly covered by one layer of flakelike products. Similar nanoflakes were also found on the base and cantilever. The nanoflakes are aligned almost perpendicularly to the local substrate and have an average length of about 1 $\mu$m. The inset of Fig. 1(a) shows a high magnification SEM image of the tip portion, in which it can be seen that the nanoflakes have very sharp tips with an average diameter of 17±5 nm. At the root of the nanoflakes, the width reaches about 100 nm. The thickness of nanoflakes varies within 10–20 nm from the tip to the root.

To investigate the chemical components of as-grown samples, XPS measurements were carried out and the O 1*s* and Fe 2*p* spectra are shown in Fig. 1(b). In the O 1*s* spectra, the peak located at 530.5 eV is ascribed to the ionic bonds in $Fe_2O_3$.[10] A shoulder at 532.3 eV is also observed from the O 1*s* spectra, which could be due to the existence of ad-

[a)]Also at: National University of Singapore, Nanoscience and Nanotechnology Initiative, 117542, Singapore.
[b)]Author to whom correspondence should be addressed; electronic mail: physowch@nus.edu.sg
[c)]Also at: National University of Singapore Nanoscience and Nanotechnology Initiative, 117576, Singapore.

 

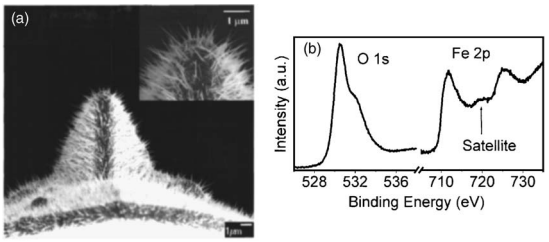


FIG. 1. (a) Typical SEM image of $\alpha$-$Fe_2O_3$ nanoflakes on an AFM tip. Inset shows a high magnification SEM image of the tip apex. (b) XPS spectra of O 1*s* and Fe 2*p* from as-grown samples.

sorbed carbon oxide due to this *ex situ* analysis. The two peaks around 711.8 eV and 725.0 eV with a satellite line are characteristic of $Fe^{3+}$ in $Fe_2O_3$ and correspond to Fe $2p_{3/2}$ and Fe $2p_{1/2}$ binding energies, respectively.[10] The line shape and the binding energy values agree with the previous reports for $Fe_2O_3$.[11]

TEM and high-resolution TEM (HRTEM) studies were carried out to investigate the microstructure of the nanoflakes. To avoid destroying the morphology of as-grown nanoflakes, a special TEM sample holder was used to allow the studying of the nanoflakes directly on an AFM tip. Figure 2(a) shows a typical TEM image taken from the front side of the cantilever. From it, the very sharp tip morphology of $\alpha$-$Fe_2O_3$ nanoflakes is observed again. From the image, it can also be observed that some nanoflakes are not fully grown, which may result from different local growth conditions compared with the long nanoflakes. Moreover, the average tip angle of a nanoflake can be estimated to be as small as 8°. Statistical measurements show that tip angle from different nanoflakes falls between 6°–10°. The typical HRTEM image and corresponding selective area electron diffraction (SAED) pattern of a nanoflake is shown in Fig. 2(b) and its inset. From them, we can see the nanoflake is single crystalline, consistent with the rhombohedral structure of hematite ($\alpha$-$Fe_2O_3$).[12] Furthermore, combining the lattice spacings and SAED pattern in Fig. 2(b), the growth of nanoflakes can be deemed as along the [110] direction, which is the dominate growth direction in most long nanoflakes.

On the basis of the above analysis, it is seen that single-crystalline $\alpha$-$Fe_2O_3$ nanoflakes have been fabricated on AFM tips by oxidizing Fe films. Since the nanoflakes have very small tip diameters and very narrow tip angles, field emission measurements were carried out to investigate the potential of $\alpha$-$Fe_2O_3$ nanoflakes as field emitters. The FE setup is schematically shown in Fig. 3. In a vacuum chamber with a pressure of about $5\times10^{-7}$ Torr, the whole AFM tip was mounted onto a steel plate as the cathode and indium-tin oxide glass coated with phosphor was employed as the anode to collect field emitted electrons. A cover glass with a thickness of 150 $\mu$m was utilized to define the gap between electrodes and to cover the whole support platform of the cantilever at the same time. Thus, only those nanoflakes on the tip and part of the cantilever were exposed for field emission study. Typical FE results are shown in Fig. 4. From Fig. 4(a) we can see that the turn-on voltage, under which a current is distinguished from noise, is as low as 500 V. Repeated experiments demonstrate that the turn-on voltage of the $\alpha$-$Fe_2O_3$ nanoflakes on AFM tips varied between 400–600 V under the same measurement conditions. On the other hand, at an applied voltage of 900 V, the emission current reaches 160 nA. Since a pointed AFM tip is able to

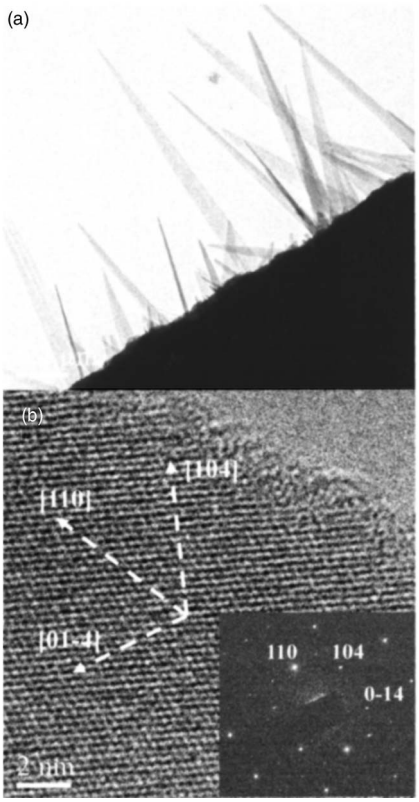


FIG. 2. (a) Typical TEM image of $\alpha$-$Fe_2O_3$ nanoflakes on an AFM tip. (b) HRTEM image from a long $\alpha$-$Fe_2O_3$ nanoflake. From it, the lattice fringe is measured as about 2.71 Å, consistent with the interplanar spacings of both (104) and $(01\bar{4})$ in $\alpha$-$Fe_2O_3$. The inset shows corresponding SAED pattern, which can be indexed with crystal zone of $[\bar{4}41]$.

enhance the local electric field and fluorescent images were also observed only in the vicinity of the apex during field emission, the emission current is deduced to originate mainly from the nanoflakes on the tip part. Estimating the emission area to be 10 $\mu m^2$ which includes tens to one hundred emitters according to the SEM image [Fig. 1(a)], a current density under 900 V is obtained as high as 1.6 A $cm^{-2}$ on the apex of the AFM tip. In addition, Fig. 4(b) shows a two-region linear dependence in the corresponding Fowler-Nordheim (FN) plots, suggesting that the tunneling emission occurs in each region. Such FE performance is comparable to the best results from CNTs and many other nanoscale emitters.[13] Hence, $\alpha$-$Fe_2O_3$ nanoflakes can provide efficient emission current. Moreover, the nanoflakes can be readily grown on the supporting structures such as the AFM tip. These properties render the $\alpha$-$Fe_2O_3$ nanoflake a potentially useful novel candidate for field emitters.

To analyze the FE behavior of $\alpha$-$Fe_2O_3$ nanoflakes on an AFM tip, the FN equation is used[14]

$$J=\frac{AF^2}{\phi}\exp(-B\phi^{3/2}/F). \tag{1}$$

Here, $J$ (A $cm^{-2}$) and $F$ (V $cm^{-1}$) are local current density and local field, respectively. $\phi$ is the work function (eV). $A$ $(1.4\times10^{-6})$ and $B$ $(6.4\times10^{7})$ are constants. Even though the electric field and current density are not constant over the emitter surface,[15] we still can define an average enhancement factor $\beta$ and an average effective emission area $\gamma$ to qualitatively analyze the emission performance

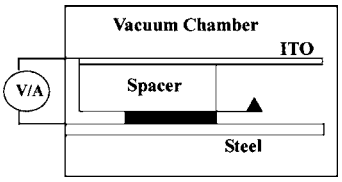


FIG. 3. Schematic of FE setup.

$$F = \beta V \text{ and } \gamma = I/J. \tag{2}$$

Combining Eqs. (2) and (1), the measured current ($I$) and voltage ($V$) in experiments can be expressed as

$$I = \frac{A\gamma\beta^2}{\phi} V^2 \exp\left(-\frac{B\phi^{3/2}}{\beta}\frac{1}{V}\right) \equiv A'V^2 \exp(-B'/V). \tag{3}$$

As mentioned above, there exits a knee point ($\sim$780 V) in the FN plots separating two regions with different slopes. Thus, Eq. (3) was used to fit the two regions separately, as shown in Fig. 4(a). We can see that the two regions follow the FN law very well, but with different fitting parameters $A' = 2.3 \times 10^{-12}$, $B' = 3010$ below the knee point and $A' = 1.6 \times 10^{-9}$, $B' = 8200$ above the knee point. From $A'$ and $B'$ values, the average enhancement factor is calculated using Eq. (3) as $\beta_1 = 2.8 \times 10^5$ cm$^{-1}$ at lower voltages and $\beta_2 = 1 \times 10^5$ cm$^{-1}$ at higher voltages. Here, the work function value of 5.6 eV for bulk $\alpha$-$Fe_2O_3$ is used.[16] The value of $\beta_1$ is quite comparable to the enhancement factor from a rope of CNTs (Ref. 17) under similar experimental conditions. On the other hand, we may use a hemisphere model[18] to obtain the enhancement factor from the morphology of emitters

$$\beta = 1/\alpha R_{\text{tip}}, \tag{4}$$

where $R_{\text{tip}}$ is the tip radius and $\alpha$ is a modifying factor determined by local geometric and electronic factors. Using the tip radius from SEM measurements and $\beta$ values mentioned above, we obtained $\alpha_1 \approx 3-5.5$ and $\alpha_2 \approx 8-14.7$. The value of $\alpha_1$ agrees with the theoretical result obtained solely from the screening due to image charges.[18] Under higher voltages, a larger $\alpha_2$ suggests the effects of screening by nearby emitters begin to play a role.[19] Thus, we argue that at low voltages, only very small numbers of nanoflakes contribute to the field emission; with the increase in voltage, more and more nanoflakes further away from the apex also contribute to electron emission. Such a gradual turn-on field emission results from the different positions of emitters on an AFM tip, in addition to the self-selectivity of emitters with different morphologies.[20] Furthermore, from Eq. (3), we can further estimate the effective emission area to be $\gamma_1 \approx 0.012$ nm$^2$ at lower voltages and $\gamma_2 \approx 60$ nm$^2$ at higher voltages. An excessively small value of $\gamma_1$ may not be true because of the uncertainty in estimation, but comparing with $\gamma_2$, it strongly suggests very few emitters in our experiments. It is possibly the different turn-on voltages for different nanoflakes which result in a nonlinear feature in FN plots, as revealed in other 1D system.[21]

In conclusion, as a preliminary work to investigate the FE properties of nanostructures, we have demonstrated that $\alpha$-$Fe_2O_3$ nanoflakes on an AFM tip have a high emission current density comparable to the best CNTs. Such excellent FE performance closely relates to their very sharp tips and perfect crystalline structures. As-grown samples on AFM tips show a nonlinear FN behavior, which could be contributed to gradual turn-on of different emitters. All of the results suggest that the aligned $\alpha$-$Fe_2O_3$ nanoflakes can be another candidate for future cold cathode devices. By further optimizing the growth, a single nanoflake may be directly fabricated on an AFM tip as a point emitter or an AFM probe.

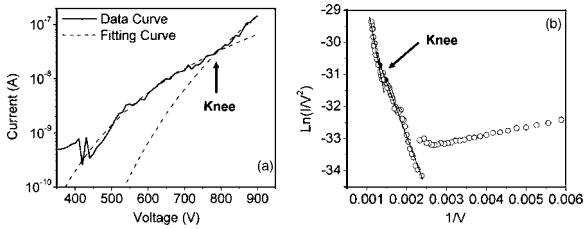


FIG. 4. (a) FE *I-V* curve and fitting curves based on FN equation. (b) FN plots corresponding to the experimental data in (a).

The authors acknowledge the support from NUS Academic Research Fund and NUS Nanoscience and Nanotechnology Initiative. One of the authors (T.Y.) acknowledges the support from the Singapore Millennium Foundation.

[1] N. de Jonge and J.-M. Bonard, Philos. Trans. R. Soc. London, Ser. A **362**, 2239 (2004).
[2] R. H. Baughman, A. A. Zakhidov, and W. A. de Heer, Science **297**, 787 (2002).
[3] J. Zhou, N. S. Xu, S. Z. Deng, J. Chen, J. C. She, and Z. L. Wang, Adv. Mater. (Weinheim, Ger.) **15**, 1835 (2003); J. J. Chiu, C. C. Kei, T. P. Perng, and W. S. Wang, *ibid.* **15**, 1361 (2003); Y. W. Zhu, H. Z. Zhang, X. C. Sun, S. Q. Feng, J. Xu, Q. Zhao, B. Xiang, R. M. Wang, and D. P. Yu, Appl. Phys. Lett. **83**, 144 (2003); V. N. Tondare, C. Balasubramanian, S. V. Shende, D. S. Joag, V. P. Godbole, and S. V. Bhoraskara, *ibid.* **80**, 4813 (2002).
[4] J. Zhang, J. Tang, G. Yang, Q. Qiu, L.-C. Qin, and O. Zhou, Adv. Mater. (Weinheim, Ger.) **16**, 1219 (2004).
[5] J. Tang, G. Yang, Q. Zhang, A. Parhat, B. Maynor, J. Liu, L.-C. Qin, and O. Zhou, Nano Lett. **5**, 11 (2005); H. Dai, J. H. Hafner, A. G. Rinzler, D. T. Colbert, and R. E. Smalley, Nature (London) **384**, 147 (1996).
[6] J. K. Leland and A. J. Bard, J. Phys. Chem. **91**, 5076 (1987).
[7] L. Huo, W. Li, L. Lu, H. Cui, S. Xi, J. Wang, B. Zhao, Y. Shen, and Z. Lu, Chem. Mater. **12**, 790 (2000).
[8] M. Catti, G. Valerio, and R. Dovesi, Phys. Rev. B **51**, 7441 (1995).
[9] Y. Xiong, Z. Li, X. Li, B. Hu, and Y. Xie, Inorg. Chem. **43**, 6540 (2004); Y. Y. Fu, J. Chen, and H. Zhang, Chem. Phys. Lett. **350**, 491 (2001).
[10] C. D. Wagner, A. V. Naumkin, A. K. Vass, J. W. Allison, C. J. Powell, and J. R. Rumble Jr., NIST X-ray Photoelectron Spectroscopy Database, Web version: ⟨http://srdata.nist.gov/xps/⟩.
[11] Y. Y. Fu, R. M. Wang, J. Xu, J. Chen, Y. Yan, A. V. Narlikar, and H. Zhang, Chem. Phys. Lett. **379**, 373 (2003); T. S. Niedrig, W. Weiss, and R. Schlögl, Phys. Rev. B **52**, 17449 (1995).
[12] JCPDS-International Center for Diffraction Data, No. 33–0664 (1995).
[13] W. Zhu, C. Bower, O. Zhou, G. P. Kochanski, and S. Jin, Appl. Phys. Lett. **75**, 873 (1999); M. Kasu and N. Kobayashi, *ibid.* **76**, 2910 (2000).
[14] R. H. Fowler and L. W. Nordheim, Proc. R. Soc. London, Ser. A **119**, 173 (1928).
[15] D. Nicolaescu, J. Vac. Sci. Technol. B **11**, 392 (1993).
[16] E. R. Batista and R. A. Friesner, J. Phys. Chem. B **106**, 8136 (2002).
[17] D. Lovall, M. Buss, E. Graugnard, R. P. Andres, and R. Reifenberger, Phys. Rev. B **61**, 5683 (2000).
[18] R. Gomer, *Field Emission and Field Ionization* (Harvard University Press, Cambridge, 1961), p. 195.
[19] P. G. Collins and A. Zettl, Phys. Rev. B **55**, 9391 (1997).
[20] J. M. Bonard, K. A. Dean, B. F. Coll, and C. Klinke, Phys. Rev. Lett. **89**, 197602 (2002).
[21] J. Chen, S. Z. Deng, J. C. She, N. S. Xu, W. Zhang, X. Wen, and S. Yang, J. Appl. Phys. **93**, 1774 (2003).